Journal of Innovative Optical Health Sciences
Vol. 7, No. 1 (2014) 1350056 (7 pages)

DOI: 10.1142/S1793545813500569





# DISTINGUISHING BETWEEN HYPERPLASTIC AND ADENOMATOUS POLYPS AND NORMAL COLONIC MUCOSA BY USING MULTIPHOTON LASER SCANNING MICROSCOPY

HONGSHENG LI*,¶, CHANGYIN FENG†,¶, ZHIFEN CHEN‡,¶, YINGHONG YANG†, WEIZHONG JIANG‡, SHUANGMU ZHUO*, XIAOQIN ZHU*, GUOXIAN GUAN‡,§ and JIANXIN CHEN*,‖

*Institute of Laser and Optoelectronics Technology
Fujian Provincial Key Laboratory for Photonics Technology
Key Laboratory of Optoelectronic Science and Technology
for Medicine of Ministry of Education
Fujian Normal University, Fuzhou 350007, P. R. China

†Department of Pathology
The Affiliated Union Hospital
Fujian Medical University, Fuzhou 350001, P. R. China

‡Department of Colorectal Surgery
The Affiliated Union Hospital
Fujian Medical University, Fuzhou 350001, P. R. China
§gxguan1108@163.com
‖chenjianxin@fjnu.edu.cn

Received 31 May 2013
Accepted 15 September 2013
Published 22 November 2013

Precisely distinguishing between hyperplastic and adenomatous polyps and normal human colonic mucosa at the cellular level is of great medical significance. In this work, multiphoton laser scanning microscopy (MPLSM) was used to obtain the high-contrast images and the morphological characteristics from normal colonic mucosa, hyperplastic polyps and tubular adenoma. By integrating the length and area measurement tools and computing tool, we quantified the difference of crypt morphology and the alteration of nuclei in normal and diseased human colonic mucosa. Our results demonstrated that the morphology of crypts had an obvious tendency to cystic dilatation or elongated in hyperplastic polyps and tubular adenoma. The content and number of mucin droplets of the scattered goblet cells had a piecemeal reduction in hyperplastic polyps and a large decrease in tubular adenoma. The nuclei of epithelial cells might be elongated



¶These authors contributed equally to the work.

and pseudostratified, but overt dysplasia was absent in hyperplastic polyps. Nevertheless, the nuclei showed enlarged, crowded, stratified and a rod-like structure, with loss of polarity in tubular adenoma. These results suggest that MPLSM has the capacity to distinguish between hyperplastic and adenomatous polyps and normal human colonic mucosa at the cellular level.

*Keywords*: Normal colonic mucosa; hyperplastic polyps; tubular adenoma.



## 1. Introduction

Colonic cancer is the fourth most common cancer in men and the third most common cancer in women worldwide.[1] Most colonic cancer arise from precursor adenomatous polyps, and there are abundant data to support an adenoma carcinoma sequence.[2] Epithelial polyps of the colon have been classified as non-neoplastic (e.g., hyperplastic polyps) and neoplastic (adenomas).[3] While tubular adenomas — because of their cytological atypia — were recognized as the precursor lesions for colorectal carcinoma, hyperplastic polyps were perceived as harmless lesions without any potential for malignant progression mainly because hyperplastic polyps are missing cytological atypia.[4] During the development of adenomatous polyps, morphological changes have been observed in the mucosal layer. Probing the alterations in normal and diseased tissues and performing real-time histology or virtual biopsy for the diagnosis of colonic cancer is of great medical significance. Although imaging approaches such as chromoendoscopy, high resolution and magnification endoscopy, narrow band imaging and auto-fluorescence imaging improve the visualization and detection of mucosal lesions, histologic examination of the targeted lesion remains the gold standard for a definitive diagnosis.[5] Gastroenterologists still rely on the results of histological diagnosis.[6] However, it is questionable that nonrepresentative biopsies may miss relevant portions of tissue, leading to underestimation of the diagnosis and a much higher risk for the patients.[7] Furthermore, with resection of benign lesions or suspicious areas, the standard approach results in a large proportion of unnecessary polypectomies, which increases time, risk and cost of colonoscopy with unnecessary follow-up.[8] Hence, today's challenge for new imaging technology is to observe morphological and pathological characteristics in normal and diseased tissues and perform real-time histology or virtual biopsy in colonic mucosal layer.

Recently, multiphoton laser scanning microscopy (MPLSM) has shown the ability to investigate unstained samples due to intrinsic sources of nonlinear signals.[9,10] MPLSM has several notable advantages over traditional optical imaging technique, such as label-free detection, low photodamage and photobleaching.[11–15] In this paper, we study normal, hyperplastic and adenomatous colonic mucosa and focus on the alterations of crypt and epithelial cell by using MPLSM based on second harmonic generation (SHG) and two-photon excited fluorescence (TPEF).

## 2. Materials and Methods

MPLSM used in this study has been described previously.[16] The system is mainly an Axiovert 200 microscope (LSM 510 META, Zeiss) equipped with a mode-locked femtosecond Ti:Sapphire laser (110 fs, 76 MHz), tunable from 700 to 980 nm (Mira 900-F, Coherent), and has been described in detail in previous publications. The beam of the laser is scanned in the focal plane by a galvanometer-driven optical scanner (Zeiss). An acousto-optic modulator was directed toward controlling the laser intensity attenuation. We employed a Plan-Apochromat 63× (numerical aperture NA = 1.4) oil immersion objective for focusing the excitation beam and for collecting the backwards signals to obtain high-resolution images. TPEF and SHG images were achieved with 810 nm excitation at 2.56 $\mu$s per pixels in the two-channel mode, one channel (387–419 nm) was to show SHG signal (green color-coded) and another channel (430–698) was used to collect TPEF signals (red color-coded). To obtain a large-area image and record the focus position, we used an optional HRZ 200 fine-focusing stage (HRZ 200, Carl Zeiss) to translate the samples after x-y scan of the samples and to record the focus position. The average laser power at the specimen was maintained at $< 5$ mW, and no photobleaching was observed at this low power level.

A total of 13 colonic tissues specimens from the Affiliated Union Hospital of Fujian Medical University are examined in this study, three are diagnosed as normal, five with hyperplastic polyps and five with tubular adenoma. The *ex vivo* colonic samples (normal tissue, hyperplastic polyps, tubular adenoma) are obtained from patients undergoing reconstructive surgical procedures. Each sample is cut into 5 $\mu$m thickness frozen section perpendicular to the axial direction by the freezing microtome, stored in a refrigerator ($-86^{\circ}$C) and sandwiched between the microscope slide and a piece of the cover grass. To avoid dehydration and shrinkage during the whole imaging process, the samples are sprinkled with phosphate buffered saline (PBS) solution (pH 7.4).

## 3. Results and Discussion

### 3.1. *Normal colonic mucosa*

MPLSM can provide cellular and subcellular microstructure imaging by excitation of tissue intrinsic fluorescent molecules.[17] In our work, TPEF signals mainly originate from nicotinamide adenine dinucleotide (NADH) and flavin adenine dinucleotide (FAD) of cell. SHG signals originate from collagen fiber with noncentrosymmetric structure. MPLSM images and the corresponding H&E light microscopic image of the normal colonic mucosa are shown in Fig. 1. As can be seen, round-shape with uniform distribution of mucous secreting glands or crypts are observed in a single view. Lamina propria [blue arrow in Fig. 1(a)] distinctly and symmetrically separates individual crypts. In Fig. 1(b), the round or oval lumen (white arrow) of the crypts appear as black holes projecting onto the surface of the mucosa, and each crypt is surrounded by a homogeneous layer of epithelial cells. The mucin-containing goblet cells (yellow arrow) and the columnar epithelial cells are readily identifiable, and black spots within the surface of the colonic mucosa represent mucin in goblet cells. Nuclei (pink arrow) of epithelial cells are obtained by MPLSM, and seen along the basement membrane. These results are confirmed by H&E staining image of biopsy specimen in Fig. 1(d).

### 3.2. *Hyperplastic polyps*

Hyperplastic polyps are by far the most common colorectal lesions and they occur most often in the distal part of the colon and rectum.[4] It is generally believed to have no correlation with adenoma and cancer development.[18] MPLSM images and the corresponding H&E light microscopic image of hyperplastic polyps are shown in Fig. 2. In hyperplastic polyps, abnormal often enlarged crypts (yellow arrow) with a tendency to cystic dilatation, disorganized appearance and juvenile serration of the epithelial lining can be seen. The space between the crypts is enlarged and the lumens of the crypts are arranged at irregular intervals [in Fig. 2(a)]. The scattered goblet cells (white arrow) are reduced in number and mucin droplets were inconspicuous. The columnar cells with abundant eosinophilic cytoplasm show irregular cell architecture. Small, matted cells that appeared in the lamina propria are considered to be inflammatory cells infiltrating the lamina propria. Nuclei of the epithelial cells may be elongated and pseudostratified, and the arrangement remains along the basement membrane, but overt dysplasia is absent. The foregoing results are correlated with H&E-stained image in Fig. 2(d).

### 3.3. *Tubular adenoma*

Tubular adenoma has a premalignant potential with a high risk for progression to colorectal cancer.[19,20] The high-contrast multiphoton images and the corresponding H&E light microscopic image of tubular adenoma are exhibited in Fig. 3. With the lack of uniform architecture, the elongated luminal opening of crypts (yellow arrow) are presented. The columnar cells are ordered in a palisade manner. Goblet cells expel their mucus and acquired further reduction in the number. Mixed inflammatory cells (white arrow) infiltration is indicated in the lamina propria. Special attention is paid to morphology of nuclei. The tubular adenoma shows enlarged, crowded and stratified nuclei (pink arrow), with loss of polarity and a rod-like structure. The foregoing characteristics indicating neoplasia can be revealed in multiphoton images that correspond well with H&E-stained microscopic image [see Fig. 3(d)].

By integrating the length and area measurement tools and computing tool, we quantified the difference of crypt morphology and the alteration of nuclei in normal colonic mucosa, hyperplastic polyps and tubular adenoma. In detail, the circumference of crypt and the area of nuclei in normal colonic mucosa are $308.4 \pm 22.6\,\mu$m and $9.6 \pm 1.8\,\mu$m$^2$ ($n = 30$ areas of 3 biopsies), in hyperplastic polyps

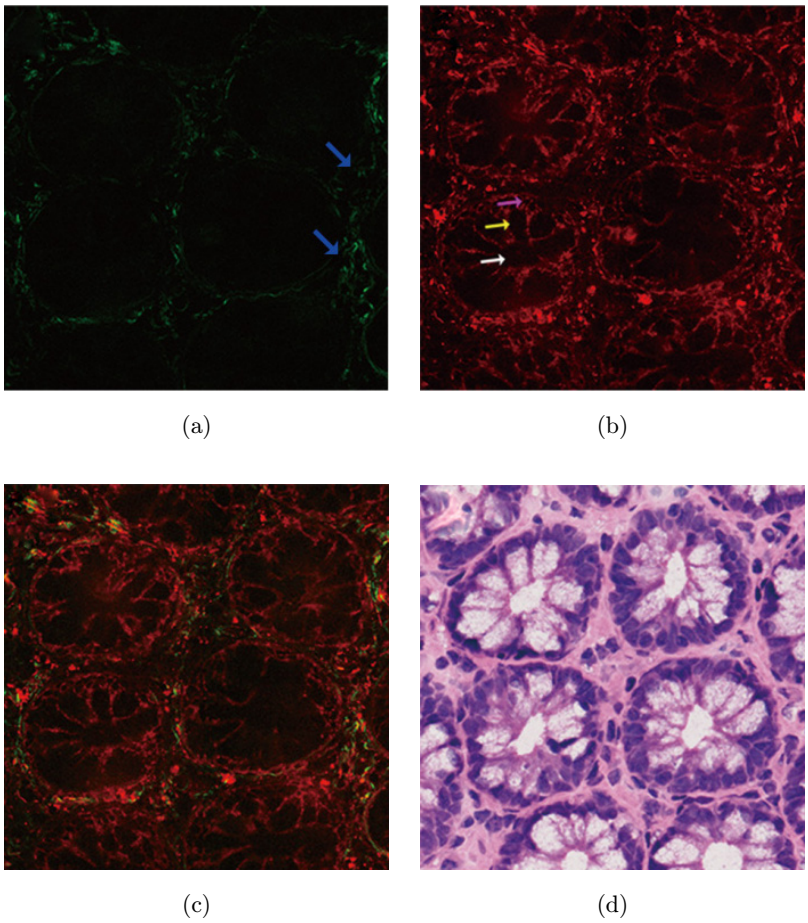

(a) (b)

(c) (d)

Fig. 1. Normal colonic mucosa. (a) SHG image (green color-coded); (b) TPEF image (red color-coded); (c) Overlay SHG/TPEF image; (d) The corresponding H&E-stained image. White arrow: crypt lumen; yellow arrow: goblet cell; pink arrow: nucleus; blue arrow: lamina propria.

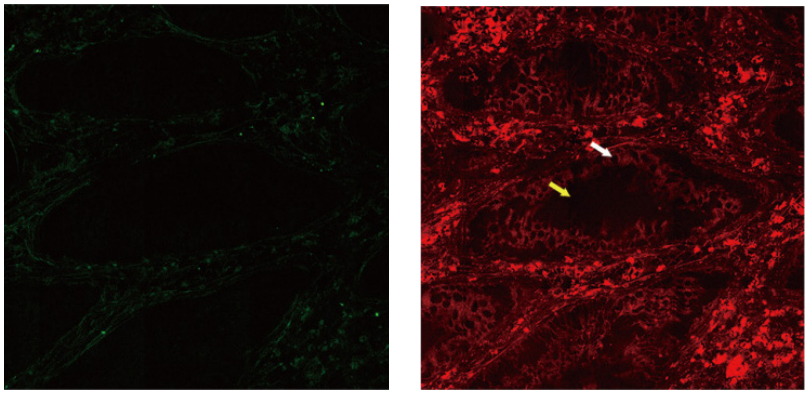

(a) (b)

Fig. 2. Hyperplastic polyps. (a) SHG image (green color-coded); (b) TPEF image (red color-coded); (c) Overlay SHG/TPEF image; (d) The corresponding H&E-stained image. Yellow arrow: cystic dilatation of crypts lumen; white arrow: decrescent mucin droplets.

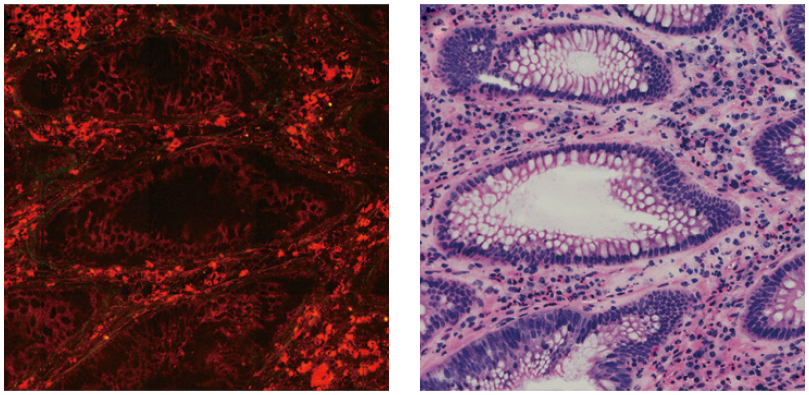

(c) (d)

Fig. 2. (*Continued*)

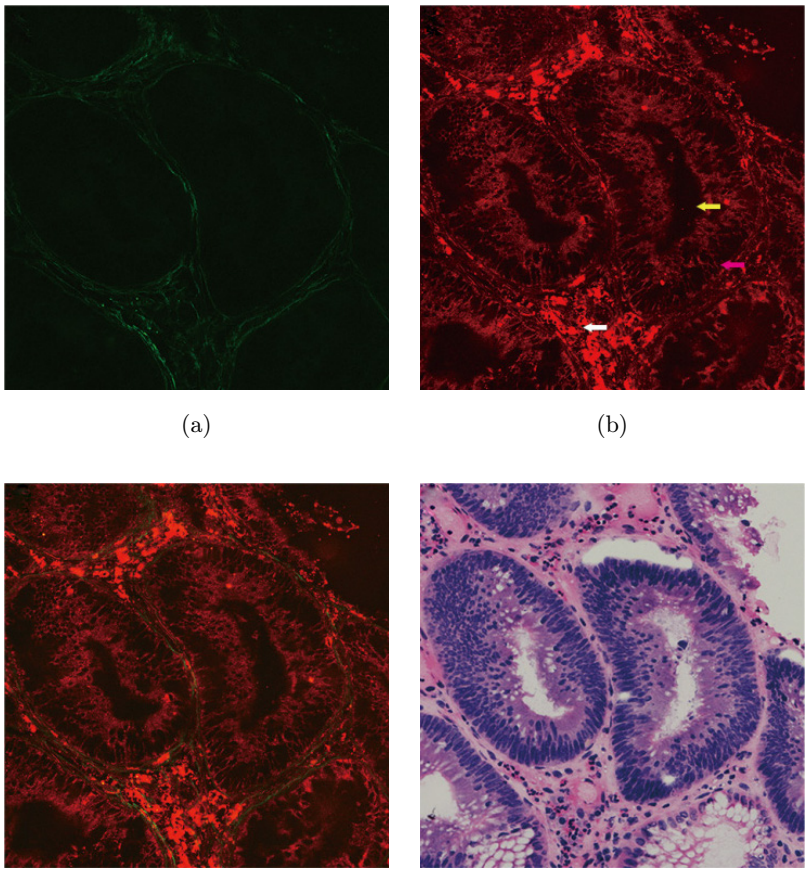

(a) (b)

(c) (d)

Fig. 3. Tubular adenoma. (a) SHG image (green color-coded); (b) TPEF image (red color-coded); (c) Overlay SHG/TPEF image; (d) The corresponding H&E-stained image. Yellow arrow: elongated luminal opening; pink arrow: rod-like structure and stratified nuclei; white arrow: inflammatory cells.

are $487.5 \pm 43.4\,\mu$m and $20.6 \pm 8.7\,\mu$m$^2$ ($n = 50$ areas of 5 biopsies), and in tubular adenoma are $669.7 \pm 83.8\,\mu$m and $44.7 \pm 14.2\,\mu$m$^2$ ($n = 50$ areas of 5 biopsies). The results suggest that the circumference of crypt and the area of nuclei in different colonic mucosa can serve as intrinsic indicators for determining normal, hyperplastic and adenomatous colonic mucosa.

## 4. Conclusion

In this study, we employed MPLSM to obtain the difference in morphology of crypts, the alterations of epithelial cells and the shape and distribution of nuclei of normal colonic mucosa, hyperplastic polyps and tubular adenoma. The findings demonstrate that MPLSM can detect and identify the different colonic mucosa at the cellular level, also suggest that the circumference of crypts and the area of nuclei can serve as intrinsic indicators for determining normal, hyperplastic and adenomatous colonic mucosa. With the application of fiber optics in microscopy and the advancement of the multiphoton-based endoscopic techniques, MPLSM will therefore allow us to perform real-time *in vivo* identification of normal, hyperplastic and adenomatous colonic mucosa at the cellular level.[21,22]

## Acknowledgment

Contract grant sponsor: National Natural Science Foundation of China; Contract grant numbers: 81271620; 61275006; 81101209; Program for Changjiang Scholars and Innovative Research Team in University; Contract grant number: IRT1115.

## References

1. M. M. Center, A. Jemal, R. A. Smith, E. Ward, "Worldwide variations in colorectal cancer," *CA Cancer J. Clin.* **59**, 366–378 (2009).
2. L. J. Burge, "Colorectal polyps and other precursor lesions: Need for an expanded view," *Gastroenterol. Clin. North Am.* **3**, 959–970 (2002).
3. B. C. Morson, "Precancerous lesions of the colon and rectum: Classification and controversial issues," *J. Am. Med. Assoc.* **179**, 316–321 (1962).
4. D. E. Aust, G. B. Baretton, "Serrated polyps of the colon and rectum (hyperplastic polyps, sessile serrated adenomas, traditional serrated adenomas, and mixed polyps) — proposal for diagnostic criteria," *Virchows Arch.* **457**, 291–297 (2010).
5. D. Moussata, "The confocal laser endomicroscopy," *Acta Endosc.* **39**, 448–451 (2009).
6. A. Hoffman, M. Goetz, M. Vieth, P. R. Galle, M. F. Neurath, R. Kiesslich "Confocal laser endomicroscopy: Technical status and current indications," *Endoscopy* **38**, 1275–1283 (2006).
7. G. D. D. Palma, "Confocal laser endomicroscopy in the "*in vivo*" histological diagnosis of the gastrointestinal tract," *World J. Gastroenterol.* **15**, 5770–5775 (2009).
8. A. M. Buchner, M. W. Shahid, M. G. Heckman, M. Krishna, M. Ghabril, M. Hasan, J. E. Crook, V. Gomez, M. Raimondo, T. Woodward, H. C. Wolfsen, M. B. Wallace, "Comparison of probe-based confocal laser endomicroscopy with virtual chromoendoscopy for classification of colon polyps," *Gastroenterology* **138**, 834–842 (2010).
9. W. R. Zipfel, R. M. Williams, R. Christie, A. Y. Nikitin, B. T. Hyman, W. W. Webb, "Live tissue intrinsic emission microscopy using multiphoton-excited native fluorescence and second harmonic generation," *Proc. Natl. Acad. Sci. USA* **100**, 7075–7080 (2003).
10. M. C. Skala, K. M. Riching, A. Gendron-Fitzpatrick, J. Eickhoff, K. W. Eliceiri, J. G. White, N. Ramanujam, "*In vivo* multiphoton microscopy of NADH and FAD redox states, fluorescence lifetimes, and cellular morphology in precancerous epithelia," *Proc. Natl. Acad. Sci. USA* **104**, 19494–19499 (2007).
11. P. T. C. So, C. Y. Dong, B. R. Masters, K. M. Berland, "Two-photon excitation fluorescence microscopy," *Annu. Rev. Biomed. Eng.* **2**, 399–429 (2000).
12. S. M. Zhuo, L. Q. Zheng, J. X. Chen, S. S. Xie, X. Q. Zhu, X. S. Jiang, "Depth-cumulated epithelial redox ratio and stromal collagen quantity as quantitative intrinsic indicators for differentiating normal, inflammatory, and dysplastic epithelial tissues," *Appl. Phys. Lett.* **97**, 173701–173704 (2010).
13. P. J. Campagnola, L. M. Loew, "Second-harmonic imaging microscopy for visualizing biomolecular arrays in cells, tissues and organisms," *Nat. Biotechnol.* **21**, 1356–1360 (2003).
14. V. A. Hovhannisyan, P. J. Su, S. J. Lin, C. Y. Dong, "Quantifying thermodynamics of collagen thermal denaturation by second harmonic generation imaging," *Appl. Phys. Lett.* **94**, 233902–233905 (2009).
15. R. Cicchi, A. Crisci, A. Cosci, G. Nesi, D. Kapsokalyvas, S. Giancane, M. Carini, F. S. Pavone, "Time- and spectral-resolved two-photon imaging of healthy bladder mucosa and carcinoma *in situ*," *Opt. Express* **18**, 3840–3849 (2010).
16. S. M. Zhuo, J. M. Chen, T. S. Luo, D. S. Zou, J. J. Zhao, "Multimode nonlinear optical imaging of the dermis in *ex vivo* human skin based on the combination of multichannel mode and Lambda mode," *Opt. Express* **14**, 7810–7820 (2006).
17. J. X. Chen, S. M. Zhuo, R. Chen, X. S. Jiang, S. S. Xie, Q. L. Zou, "Depth-resolved spectral imaging of rabbit oesophageal tissue based on two-photon excited fluorescence and second-harmonic generation," *New J. Phys.* **9**, 212 (2007).
18. M. Koike, K. Inada, H. Nakanishi, A. Matsuura, S. Nakamura, M. Tatematsu, "Cellular differentiation status of epithelial polyps of the colorectum: The

gastric foveolar cell-type in hyperplastic polyps," *Histopathology* **42**, 357–364 (2003).

19. S. J. Winawer, M. J. O'Brien, J. D. Waye, O. Kronborg, J. Bond, P. Frühmorgen, L. H. Sobin, R. Burt, A. Zauber, B. Morson, "Risk and surveillance of individuals with colorectal polyps. Who Collaborating Centre for the prevention of colorectal cancer," *Bull. World Health Organ* **68**, 789–795 (1990).
20. K. Wallace, J. A. Baron, M. R. Karagas, B. F. Cole, T. Byers, M. A. Beach, L. H. Pearson, C. A. Burke, W. B. Silverman, R. Sandler, "The association of physical activity and body mass index with the risk of large bowel polyps," *Cancer Epidemiol. Biomarkers Prev.* **14**, 2082–2086 (2005).
21. K. Melican, A. Richter-Dahlfors, "Real-time live imaging to study bacterial infections it *in vivo*," *Curr. Opin. Microbiol.* **12**, 31–36 (2009).
22. B. A. Flusberg, E. D. Cocker, W. Piyawattanametha, J. C. Jung, E. L. M. Cheung, M. J. Schnitzer, "Fiber-optic fluorescence imaging," *Nat. Methods* **2**, 941–950 (2005).